Dissociation and internal excitation of molecular nitrogen due to $N + N_2$ collisions using direct molecular simulation

Maninder S. Grover* and Thomas E. Schwartzentruber†
Department of Aerospace Engineering and Mechanics, University of Minnesota, Minneapolis, MN 55455, USA.
Richard L. Jaffe‡
NASA Ames Research Center, Moffett Field, California 94035, USA

In this work we present a molecular level study of N_2+N collisions, focusing on excitation of internal energy modes and non-equilibrium dissociation. The computation technique used here is the direct molecular simulation (DMS) method and the molecular interactions have been modeled using an $ab-initio$ potential energy surface (PES) developed at NASA's Ames Research Center. We carried out vibrational excitation calculations between 5000K and 30000K and found that the characteristic vibrational excitation time for the $N + N_2$ process was an order of magnitude lower than that predicted by the Millikan and White correlation. It is observed that during vibrational excitation the high energy tail of the vibrational energy distribution gets over populated first and the lower energy levels get populated as the system evolves. It is found that the non-equilibrium dissociation rate coefficients for the $N + N_2$ process are larger than those for the $N_2 + N_2$ process. This is attributed to the non-equilibrium vibrational energy distributions for the $N + N_2$ process being less depleted than that for the $N_2 + N_2$ process. For an isothermal simulation we find that the probability of dissociation goes as $1/T_{tr}$ for molecules with internal energy (ϵ_{int}) less than $\sim 9.9eV$, while for molecules with $\epsilon_{int} > 9.9eV$ the dissociation probability was weakly dependent on translational temperature of the system. We compared non-equilibrium dissociation rate coefficients and characteristic vibrational excitation times obtained by using the $ab-initio$ PES developed at NASA's Ames Research Center to those obtained by using an $ab-initio$ PES developed at the University of Minnesota. Good agreement was found between the macroscopic properties and molecular level description of the system obtained by using the two PESs.

I. Introduction

Flows generated during atmospheric re-entry of vehicles involve strong thermal and chemical non-equilibrium with shock layer temperatures reaching thousands of degrees kelvin. Such extreme conditions make the modeling of such flows a great challenge. Computational tools like computational fluid dynamics (CFD) and direct simulation Monte-Carlo (DSMC) are often used to characterize these flows and are vital tools for designing the thermal protection system (TPS) for the vehicle. Current thermo-chemical models in CFD and DSMC rely on experimental data. Unfortunately, the experimental data has limitations. For example, the experimental data only goes up to 15000K[1] and comes with inherent uncertainties. This makes extrapolations based on experimental data questionable. Furthermore, there are great differences in the dissociation rates provided by experimentalists, with dissociation rate coefficients varying over orders of magnitude.[1,2]

An alternative is to employ computational chemistry methods to derive these physical quantities. In this approach, first a potential energy surface (PES) is computed by solving the electronic Schrödinger equation.

*Research Assistant, University of Minnesota, Student Member AIAA.
†Associate Professor, University of Minnesota, Senior Member AIAA
‡Research Scientist, NASA Ames Research Center, Associate Fellow AIAA.

The single point energies obtained from these calculations are then interpolated using advanced methods.[3,4,5] This results in a smooth analytic hypersurface, over which energy gradients can be calculated. Once the PES is constructed and the single point energies have been interpolated, a large number of quasi-classical trajectory (QCT)[6,7] calculations are done to determine collision cross sections, dissociation probabilities and energy transition probabilities. These rates are then incorporated in master equation (ME) analysis to generate state-to-state models.[7,8,9,10,11] While this is a powerful approach and is free of empiricism, it becomes easily intractable. For instance, if one accounts for all possible ro-vibrational state transitions, there are about $O(10^7)$ possible transitions for the $N + N_2$ system and about $O(10^{14})$ possible transitions for the $N_2 + N_2$ system making a fully resolved state-to-state model infeasible.

In this work, we use the direct molecular simulation (DMS) approach. The DMS method is essentially like the DSMC method for gas flows, but in DMS, all stochastic collision models are replaced with trajectory integration using a PES. This method was first introduced by Koura[13,14,15] as classical trajectory calculation DSMC (CTC-DSMC) and extended to rotating and vibrating molecules by Valentini, Norman and Schwartzentruber.[16,17] Similar to DSMC, the DMS method randomly forms collision pairs from the molecules present in a given volume. Hence we do not have to worry about all possible state-to-state transitions for a given gas, rather only the transitions that are dominant are simulated as the system evolves. This makes the DMS method free of any empiricism and computationally tractable. More details of the DMS method are discussed in section IIA.

Previous work done in the research group entailed studying the evolution $N_2 + N_2$ system (N4) in an isothermal heat bath[19] using a N4 PES generated by Paukku *et al.*[4] and a comparative study for the N4 system[20] was done using a PES developed by Jaffe *et al.*[3] at NASA's Ames Research Center that showed a remarkable similarity between the non-equilibrium dissociation rates and non-equilibrium internal energy distributions obtained from using the two independently generated $ab-initio$ PESs. The $N + N_2$ system has been studied by Valentini *et. al.*[21] using the PES developed by Paukku *et. al.*, here we will extend a similar analysis for the $N + N_2$ system using the PES developed by Jaffe *et. al.* at NASA Ames Research Center.

II. Simulation Method and Conditions

A. Direct Molecular Simulation

A detailed description of the DMS method has been given in prior publications,[17,19] here we will provide a brief overview for clarity. As stated above, the DMS method is basically like the DSMC method[12] but with the stochastic collision models replaced with trajectory calculations performed on a PES. In contrast to QCT based methods using master equation analysis, in the DMS method, the trajectory calculations are embedded into a time-accurate flow field calculation. Following this approach, trajectories are calculated at every time-step and the post collision state of a molecule becomes its state for the next trajectory. Therefore DMS can be used to simulate transient flows[17,18] and can resolve non-Boltzmann energy distributions within the flow.[17,18,19,20,21]

Just like DSMC, DMS only simulates a fraction of the total particle population present in the system. However, there are enough simulated particles to resolve the local distribution functions of the flow. A simulated particle, hence is a representative particle for a large number of identical real particles (W_p). The simulation is done over time steps of the order of the local mean collision time (τ_c). Over each time step particles are moved without any interaction, then collision pairs are locally selected in a cell which has the dimension of the order of a mean free path (λ_c). Once the collision pairs are selected, impact parameters and orientations of the colliding molecules are randomized and finally the trajectory is executed.

For the zero-dimensional study presented in this paper, particle movement is not required and only a single flow volume is considered. The volume dimensions were chosen such as for a given population of particles, the particle weight was unity ($W_p = 1$) for a given density and number of particles simulated. The simulation advanced with time-steps chosen as, $\Delta t_{DMS} = \tau_c/100$. At every time step random pairs of particles are selected, which in our case can be a pair of $N_2 + N_2$, $N_2 + N$ or $N + N$ pairs. A major difference here from DSMC, is that instead of having phenomenological probabilistic models determine the collision rate and collision outcomes, trajectory calculations are done over a specified PES. The outcomes of the trajectories

determine the post collision state of the molecules and this becomes the state of the molecule for the next interaction. Hence, the PES is the only chemistry input for the DMS method.

B. Collision Rate

At every DMS time step a fraction of the simulated particles (molecules and atoms) are chosen for the trajectory calculations to correspond to a conservative estimate for the collision rate in the gas. The no time counter (NTC) collision rate model[12] commonly used in DSMC is employed to form collision pairs. The hard-sphere cross section (σ) for the NTC algorithm is set to be consistent with the maximum impact parameter (b_{max}) and is given by the equation:

$$\sigma = \pi b_{max}^2 \ . \tag{1}$$

The exact equations used in DMS to select particle pairs for trajectories have been detailed in earlier work.[19,21] It has been shown in great detail that the exact value of the maximum impact parameter has no effect on the solution as long as it is chosen conservatively.[17,18] This makes it possible to have a single value for the cross section for all trajectory pairs. Keeping in mind the work done by Bender *et al.*[5] the value of b_{max} was set to:

$$b_{max} = 6\mathring{A} \tag{2}$$

C. Potential Energy Surfaces and Trajectories

Once the collision pairs are selected using the NTC method, trajectory calculations are carried out for the pairs in a manner similar to the QCT method. This has been explained in great detail in earlier DMS work presented by the group.[19,20,21] The trajectories are initialized with a random impact parameter ranging from $0 \leqslant b^2 \leqslant b_{max}^2$ and a random orientation for the molecules. Then the phase-space coordinates for all nitrogen atoms involved are progressed in time and the trajectory is integrated using the velocity Verlet scheme.[22] The time step for the trajectory integration was conservatively set to $0.05fs$. The velocity Verlet scheme integrates the equation:

$$F = m\ddot{\vec{r}} = -\nabla_r V(r) \ , \tag{3}$$

Here, r is the atomic position vector, m is the mass of the atom and $\nabla_r V(r)$ is the gradient of the PES which gives the force acting on the atom. The trajectory is integrated until the minimum separation between atoms (not bonded in the same molecule) becomes greater than $15\mathring{A}$. The atomic positions and velocities are available both pre- and post- collision for post processing and backing out quantities like internal energy. It is important to note that for a molecule, the post collision atomic positions and velocities relative to center of mass, are stored and become the initial state of the molecule for the next trajectory. Therefore no decoupling of rotational and vibrational energy is performed during a DMS calculation.

After a trajectory is completed, if atoms belonging to a molecule are greater than $6\mathring{A}$ apart then the molecule is considered dissociated. These dissociated atoms are kept in the system to be part of future trajectories. Additionally, during trajectory integration for some particle configurations the atoms may go over free energy minima in the PES resulting in new bonds being formed and others being severed. Hence, the DMS method automatically accounts for exchange reactions and no special treatment for the exchange process is required.

Since, in this work we discuss isothermal cases of excitation and relaxations, the trajectory calculations are only done for the $N_2 + N_2$ and $N_2 + N$ collision pairs. For the $N + N$ pairs, the velocity is simply sampled from a Boltzmann distribution at the given translational temperature. In earlier work done by the group[21] the $N_2 + N$ trajectory calculations were done by using N4 PES and displacing one of the atoms to a very large distance. For that work PES developed by Paukku *et al*[4] was used. In this work both $N_2 + N$(N3)[23,24] and $N_2 + N_2$ (N4)[3] systems have a dedicated ground state $ab - initio$ PES that was developed for that particular collision pair by Jaffe *et al* at NASA's Ames Research Center. A portion of this work will focus on

comparing the excitation and dissociation rates obtained from the two high fidelity $ab-initio$ PESs using the DMS method. The PESs developed by Jaffe *et al.* will be referred as "Ames Potential" and the PES developed by Paukku *et al.* will be referred as "UMN Potential" for the rest of the paper.

D. Division of Internal Energy

As described in the above section (Sec: IIC) the DMS method works only on the basis of velocities and positions of atoms involved in the trajectory. Consequently, there is no a-priori assumption of decoupling of rotational and vibrational modes of internal energy. Further, since we are using a ground state PES in this work, there is no electronic mode of internal energy. The positions and velocities of atoms in a bound molecule are used in post processing to determine total internal energy of the molecule. In this work, we did divide the internal energy of the system into vibrational and rotational modes. This was done only as a post processing step to determine the average energy associated with vibration and rotation, providing an analog to historically used terms of rotational and vibrational temperatures.[25,26]

The internal energy splitting method called vibrational prioritized framework is used here. This method was proposed by Jaffe[27] and has been widely used in the community.[5,10] The division of internal energy under this framework can be shown as:

$$\epsilon_{vib}(v) = \epsilon_{int}(v, 0) \tag{4}$$

and

$$\epsilon_{rot}(j) = \epsilon_{int}(v, j) - \epsilon_{int}(v, 0) \ . \tag{5}$$

Where $\epsilon_{int}(v, j)$ is the total internal energy of a molecule, $\epsilon_{vib}(v)$ is the energy in the vibrational mode and $\epsilon_{rot}(j)$ is the energy in rotational mode. It should be noted that this division of internal energy is arbitrary and is one of many frameworks to split the internal energy.[27] For the rest of the paper, the average value of the vibrational energy is represented by the vibrational temperature (T_{vib}) and the average rotational energy of the system is represented by the rotational temperature (T_{rot}). Where, T_{vib} and T_{rot} are given by :

$$T_{vib} = \langle \epsilon_{vib} \rangle / k_B \tag{6}$$

and

$$T_{rot} = \langle \epsilon_{rot} \rangle / k_B \ . \tag{7}$$

E. Isothermal Relaxations

In an earlier work we have discussed internal energy transfer and dissociation process for $N_2 + N_2$ collisions[20] under isothermal conditions. In this work we have first performed a similar analysis for the $N + N_2$ (Sec:IIIA, IIIB) collisions and then analyzed the system for the combined $N + N_2$ and $N_2 + N_2$ collisions occurring concurrently (Sec:IIIC, IIID). All work presented in this paper is done under isothermal conditions. The constant translational temperature was maintained by sampling the particle's (both molecules and atoms) center of mass velocities from the Maxwell-Boltzmann distribution of the desired temperature after each DMS time step.

An example result for an isothermal relaxation done using DMS is shown in Fig 1(a). In this example the gas is initialized with $T_{tr} = T_{rot} = T_{vib} = 30000K$ and the translational temperature is kept constant at $T_t = 30000K$. The density was set to $\rho = 1.28kg/m^3$ and at $t = 0$, the box only has molecular nitrogen. As the system evolves, molecules dissociate. Initially, the dissociation is primarily due to $N_2 + N_2$ collisions as the population of atomic nitrogen increases $N_2 + N$ collisions start playing an important role in the

dissociation process. Since recombination is not modeled, the system progresses until all molecules have dissociated and the system comprises of atomic nitrogen only.

Due to dissociation, the population of higher vibrational and rotational levels are depleted and there is a loss of energy in the rotation and vibrational modes, which manifests in lowering of vibrational and rotational temperatures. Eventually, the inelastic collision processes catch up with the loss of energy due to dissociation. This leads to formation of a Quasi-Steady State (QSS), here the distribution of energy in the vibrational and rotational modes becomes time invariant. These time invariant, non-equilibrium distributions can be seen in Fig: 2(a), 2(b). These depleted, time invariant distributions manifest themselves macroscopically as lowered but constant vibrational and rotational temperatures. Additionally, the distribution of total internal energy in QSS can be seen in 2(c). It should be noted that the QSS is solely a function of the translational temperature and is independent of the initial state of the gas as can be seen in Fig. 1(b).

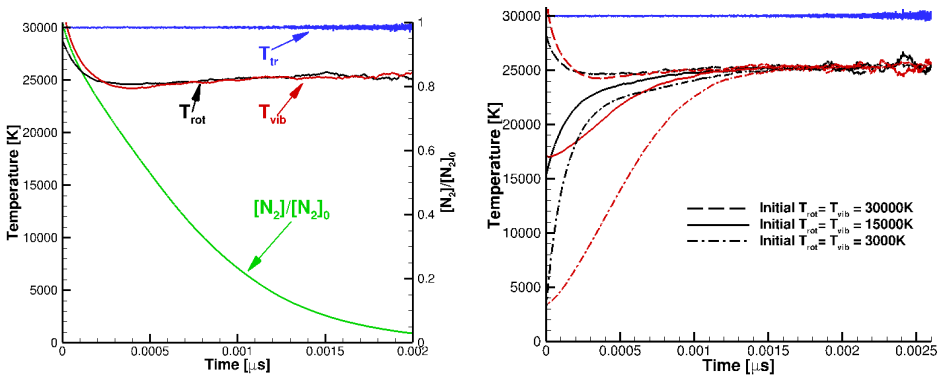

(a) Temperature and composition history of an isothermal relaxation in a box for the N3 and N4 processes .

(b) QSS for combined N3 and N4 processes with various initial internal energy states of the gas.

Figure 1. Examples of isothermal relaxation in a box and formation of the QSS for the combined N3 and N4 processes.

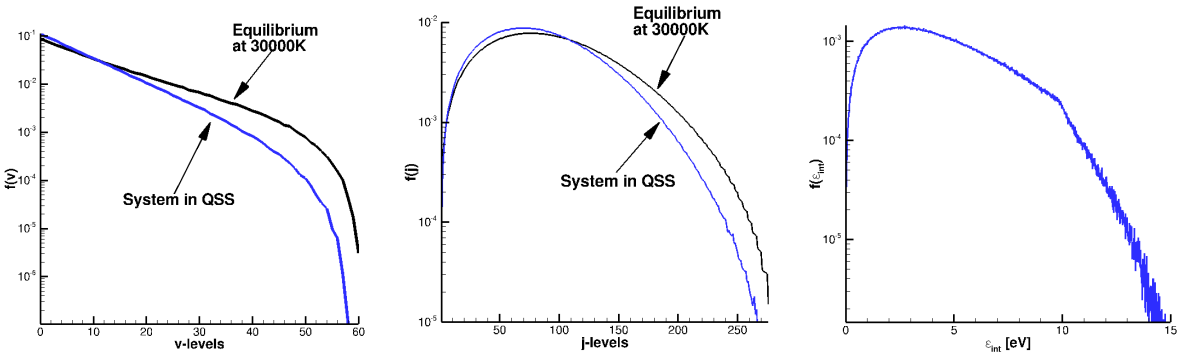

(a) Vibrational Energy Distribution in QSS.

(b) Rotational Energy Distribution in QSS.

(c) Internal Energy Distribution in QSS.

Figure 2. Internal energy distributions of N_2 molecules in QSS for $T_t = 30000K$.

III. Results

A. Vibrational excitation due to $N + N_2$ collisions

In this section we discuss the effect of atom-molecule collisions on the vibrational excitation of the gas. Isothermal vibrational excitation is carried out for translational temperatures ranging from $T_{tr} = 5000$K to $T_{tr} = 30000$K. For all cases the initial conditions are generated such that at $t = 0$, $T_{vib} = T_{rot} = 3000$K,

density was set to $\rho = 1.28kg/m^3$, the particle weight is set to unity ($W_p = 1$) and 8×10^6 DMS particles are incorporated.

In DMS random collision pairs are selected from the simulation domain. To isolate the effect of $N + N_2$ collisions, the partial density of molecular nitrogen (ρ_{N_2}/ρ_{total}) is reduced until the characteristic excitation time becomes independent of the partial density of molecular nitrogen. To determine the effect of ρ_{N_2}/ρ_{total} on characteristic excitation time, a series of excitation calculations was run with ρ_{N_2}/ρ_{total} varying from 1 to 0.001. For these calculations, at $t = 0$, $T_{vib} = T_{rot} = 3000$K and $T_{tr} = 30000$K. Fig: 3 shows the characteristic vibrational excitation time as function of the partial density of nitrogen. As can be seen from the figure, the characteristic vibrational excitation time is independent of the partial density of nitrogen for $\rho_{N_2}/\rho_{total} \leq 0.05$. To be conservative, the work presented in this section uses $\rho_{N_2}/\rho_{total} = 0.01$. Hence, in a simulation of 8×10^6 DMS particles $\sim 40,200$ are molecular nitrogen with the remainder being atomic nitrogen.

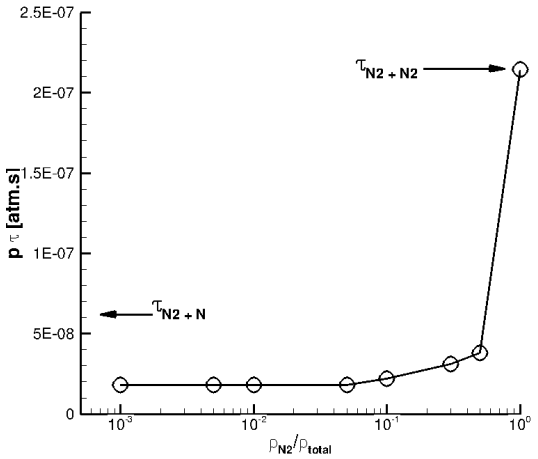

Figure 3. Dependance of characteristic excitation time on partial density of molecular nitrogen.

Fig: 4(a) shows an example of an excitation simulation. In the example, the blue curve represents the translational temperature, the black curve is the rotational temperature and the red curve is the vibrational temperature. The green curve shows the fraction of the molecular nitrogen present, with respect to the initial amount of nitrogen in the system. A Landau-Teller type expression is fitted to the red curve to give the characteristic vibrational excitation time (τ_{vib}). For cases with $T_{tr} \leq 10000$K vibrational temperature equilibrates with translational temperature before dissociation becomes prominent. However, for cases with $T_{tr} > 10000$K, there is significant dissociation before the internal energy modes attain a steady state. For these cases the relaxation of internal energy is strongly coupled with dissociation.

Fig: 4(b) shows the vibrational excitation mechanism at the molecular level for the case presented in Fig: 4(a). The solid purple curve shows the vibrational distribution system at $t = 0$, the solid blue curve shows the distribution function at QSS and the solid black curve shows the equilibrium vibrational distribution at 30000K. The symbols show instantaneous vibrational distribution functions at various times. One can see, as the vibrational excitation begins, initially, there is an over population of the high energy tail as seen at t=$\tau/8, \tau/4, \tau/2$. As the system progresses, the lower energy levels get populated until eventually the system reaches the QSS distribution.

Millikan and White correlations for vibrational excitation[29] were among the first to characterize the vibrational excitation phenomenon. The correlation was made for non-reactive collision partners. Later corrections were made to the Millikan and White formulation by Park *et al.*[30] to make the correlation appropriate for high temperature conditions by limiting the excitation rates. In Fig 5 we compare the characteristic relaxation time obtained from the DMS method (blue curve with circular symbols) with the corrected Millikan-White correlation (black curve). It can be seen that the characteristic vibrational time obtained from the DMS calculations is an order of magnitude lower than the predictions made using the Millikan and White correlation. The results are remarkably close to earlier DMS work done in the group by Valentini *et al.*[21] using the UMN PES.[4] Additionally, there is good agreement with other contemporary results obtained

by Panesi *et al.*[10] and Kim and Boyd.[11] Further investigation is required to understand the difference in the characteristic excitation time at high temperatures between the work done by Panesi *et al.* and the work presented in this paper.

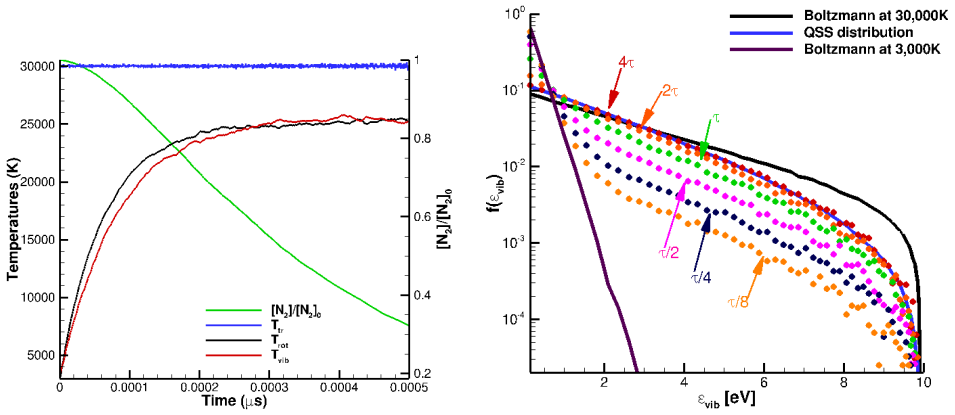

(a) Temperature and composition history for an excitation calculation.

(b) Evolution of the vibrational distribution function for the case in Fig: 4(a).

Figure 4. Examples of vibrational excitation calculations.

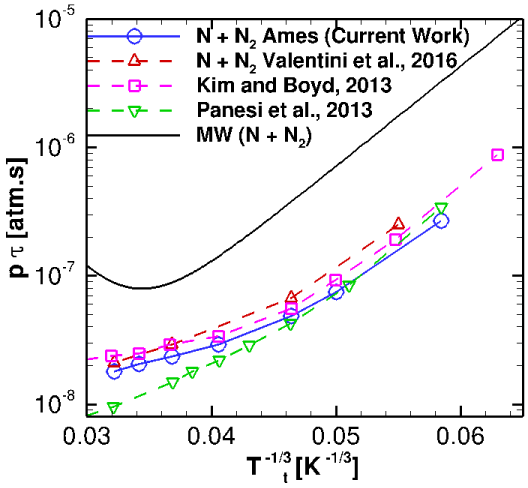

Figure 5. The figure shows the comparison of characteristic vibrational time obtained from DMS (blue curve) against Millikan and White formulation (black curve) and contemporary results[21,11,10]

B. Non-equilibrium dissociation due to $N + N_2$ collisions

In this section we discuss dissociation due to $N + N_2$ collisions. As described in the previous section (Sec:IIIA), to isolate the effects of atom-molecule collisions in DMS, the partial density of molecular nitrogen (ρ_{N_2}/ρ_{total}) was reduced so that $N + N_2$ collisions dominate. Similar to Sec:IIIA, for the DMS simulations $\rho_{N_2}/\rho_{total} = 0.01$ was used with 8×10^6 DMS particles and the particle weight was set to unity ($W_p = 1$). The molecules in the system were initialized to $T_{rot} = T_{vib} = T_{tr}$ and simulations were carried out for $T_{tr} = 10000K, 15000K, 20000K, 25000K$ and $30000K$. An example of such a calculation can be see in Fig. 7(a). Once the system is in QSS, dissociation rate constants are calculated by fitting composition histories to the following equation:

$$\frac{d[N_2]}{dt} = -k_d^{N_2+N_2}[N_2]^2 - k_d^{N+N_2}[N][N_2] \ . \tag{8}$$

Since, $[N_2] << [N]$ we can ignore the first term on Eq:8. Additionally since, at $t = 0$, $[N_2] << [N]$ it can be assumed that the concentration of atomic nitrogen does not change significantly with time and is considered to be constant. Therefore, $[N](t) \sim [N](t = 0) = [N]_0$. This further simplifies Eq:8 to a psuedo-first order rate law given by:

$$\frac{d[N_2]}{dt} = -[N]_0 k_d^{N+N_2} [N_2] \ , \tag{9}$$

which can be integrated to give:

$$[N_2](t) = [N_2]_0 exp(-k_d^{N+N_2} [N]_0 t) \ . \tag{10}$$

QSS composition histories obtained from DMS were fitted to Eq:10 to back out dissociation rate constants for the $N + N_2$ collisions ($k_d^{N+N_2}$). Fig: 6 shows the non-equilibrium dissociation rate constants obtained in this manner. In Fig 6 we compare current results with dissociation rate constants obtained from earlier DMS study done by coworkers[21] using the UMN Potential. There is remarkable agreement between the dissociation rate constants that are obtained from the DMS method using two independently developed $ab - initio$ PESs. Additionally, we have compared the experimental dissociation rate coefficients obtained by Appleton *et al.*[1] and those obtained by Hanson and Baganoff.[2] The curve fit from these experiments can be seen in Fig 6 as the solid black curve and the dashed black curve respectively, the symbols on the curves represent the temperature range over which the experiments were conducted.

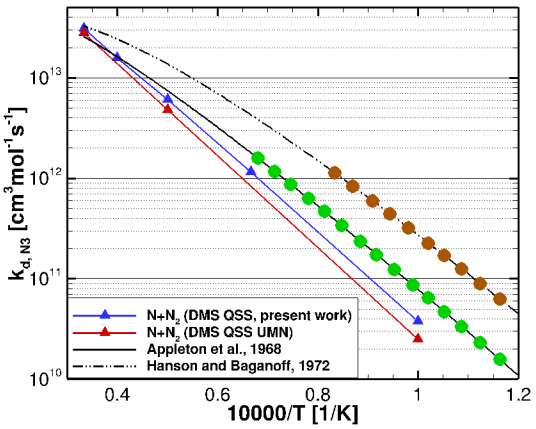

Figure 6. Comparison of non-equilibrium dissociation rate constants obtained for $N + N_2$ collisions using the DMS method using the Ames PES (blue) and the UMN PES (red). Along with rate coefficients from experiments.[1,2] The black lines represent the extrapolation obtained from the experimental data and the circular symbols show the range of experimental data.

The DMS method provides insight into the dissociation process at the molecular level as well, because the method provides the distribution of internal energy of the molecules in the simulation. Fig. 7(b) gives an example of such a distribution taken for a case with $T_{tr} = 30000K$ (shown in Fig. 7(a)). The red curve shows the distribution of internal energy ($f(\epsilon_{int})$) of the system in QSS and the blue curve shows the distribution of internal energy for the molecules that have dissociated ($f_d(\epsilon_{int})$) while the system was in QSS. The blue curve peaks at $\epsilon_{int} \sim 9.9eV$, which corresponds to the well-depth for the diatomic potential at $j = 0$. Similar distribution curves were made for $T_{tr} = 10000K, 15000K, 20000K$ and analysis of the distribution curves allowed us to construct dissociation probabilities for a given internal energy and translational temperature seen in Fig. 8.

Fig. 8 shows the QSS dissociation probability at a given internal energy for translational temperatures ranging from 10000K to 30000K. It is observed that for $\epsilon_{int} < 9.9eV$ the probability of dissociation rises from left to right. Further, the rate of the rise (slope) of the dissociation probability goes as $1/T_{tr}$. All the dissociation probability curves become closely banded and relatively flat for $\epsilon_{int} > 9.9eV$. This shows that the probability of dissociation become less dependent on translational temperature for molecules with $\epsilon_{int} > 9.9eV$.

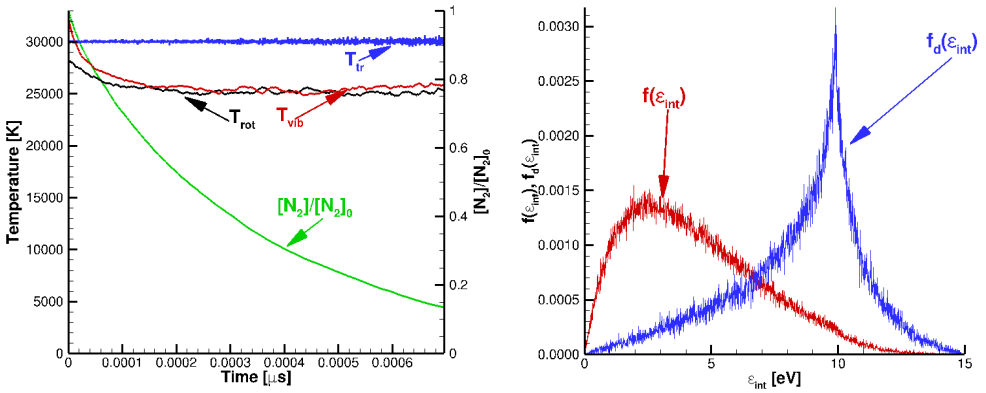

(a) Example of a dissociation calculation with $T_{tr} = 30000K$

(b) Example distribution of internal energy of molecules in QSS($f(\epsilon_{int})$) and distribution of molecules that dissociated in QSS ($f_d(\epsilon_{int})$) for the case shown in 7(a)

Figure 7. Composition and temperature profiles during a dissociation calculation, along with the internal energy distribution for the calculation.

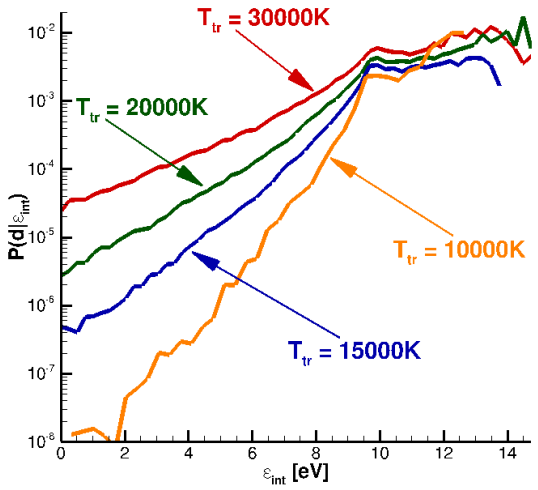

Figure 8. Dissociation probability in QSS for given internal energy and translational temperature.

For the PES used,[3,23,24] the well depth of the diatomic potential for $j = 0$ is $\sim 9.89eV$. Hence the molecules with $\epsilon_{int} > 9.9eV$ are quasi-bound. From Fig. 8 one can conclude that the probability of dissociation of quasi-bound molecules is weakly dependent on the average translational energy (T_{tr}) and consequently on the translational energy of the collision partner of the quasibound molecule. However, since there are strong temperature dependent trends until the internal energy is less than the diatomic potential energy well, it can be concluded that the dissociation process and the vibrational energy mode are heavily coupled.

In Fig. 9 we have compared the non-eqilbrium dissociation rate coefficients obtained for the $N+N_2$ collisions to that obtained for N_2+N_2 collisions in earlier work.[19,20] One can see that the dissociation rate coefficients for the $N+N_2$ collisions are higher than those for N_2+N_2 collisions. The reason behind this difference can be explained by Fig 10

Fig. 10 shows the QSS vibrational energy distributions obtained for the system at $T_{tr} = 30000K, 20000K, 15000K, 10000K$ obtained with $N + N_2$ (N3) collisions and compares them with QSS vibrational energy distributions obtained with N_2+N_2 (N4) collisions. We see that the distributions for the N3 process are less depleted from the equilibrium distribution than those obtained for the N4 process. This higher population

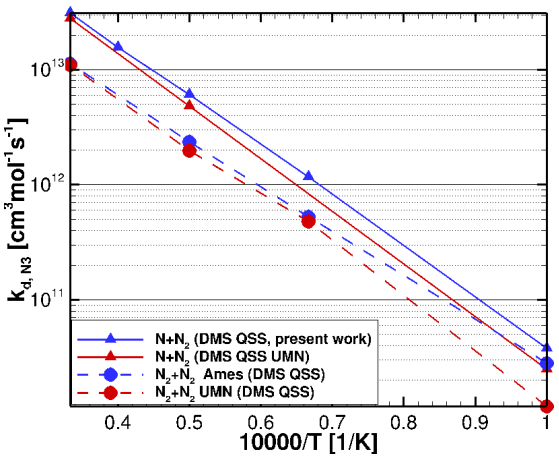

Figure 9. This figure compares non-equilibrium dissociation rate coefficients obtained for $N + N_2$ and $N_2 + N_2$ obtained from the DMS method using PESs developed at NASA Ames Research Center (blue) and the University of Minnesota (red)

at the high energy tail is caused by the fact that $N + N_2$ collisions have a high probability of resulting in exchange reactions and these exchange reactions are efficient at transporting energy across energy levels.[21] The higher population at the high energy tail results in more molecules having enough energy to dissociate and consequently a higher dissociation rate coefficient than the N4 process. This phenomenon was observed in the earlier work done in the group by Valentini *et al.*[21] using the UMN PES. The table below provides a comparison for the non-equilibrium dissociation rate coefficients obtained from the Ames PES and UMN PES.

Temperature (K)	$k^{N3}_{d-Ames}/k^{N3}_{d-UMN}$	$k^{N4}_{d-Ames}/k^{N4}_{d-UMN}$
10000	1.50	2.37
15000	-	1.09
20000	1.26	1.19
30000	1.10	1.04

C. Comparison of N4 system to N3 + N4 system

We have characterized the N4 system for the Ames potential in earlier work[20] and in the sections above we have discussed in detail the N3 system for the Ames potential. In this section we will discuss isothermal relaxation for a box filled with molecular nitrogen in which we allow both N3 and N4 processes to occur concurrently and compare this to earlier work done only for the N4 process.[20] An example of an isothermal relaxation with the N3+N4 system has been shown in Fig. 1(a).

Fig. 11 shows the comparative composition history of the isothermal relaxations with the N4 and N3+N4 systems. The comparative isothermal relaxations are carried out for $T_{tr} = 30000K, 20000K$ and $15000K$. One can see that the initial dissociation rate in each case corresponds to the dissociation rate for the pure N4 system. However, once the concentration of molecular nitrogen drops to roughly 90% of the original concentration ($[N_2]/[N_2]_0 = 0.9$) the system deviates from the pure N4 behavior and dissociation becomes faster, a result of the dissociation process being faster when N atoms are present.(Sec. IIIB.)

D. Comparison of Ab-initio Results

In the sections above (Sec. III A and Sec. III B) we have shown that the characteristic excitation times and the non-equilibrium dissociation rates obtained with the Ames PES and UMN PES for the N3 process are agree remarkably well. Further, in earlier work[20] we have shown agreement between dissociation rates for

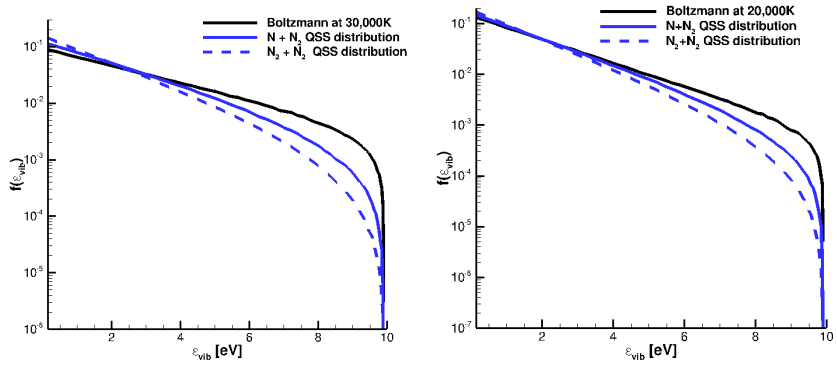

(a) $T_{tr} = 30000K$. (b) $T_{tr} = 20000K$.

(c) $T_{tr} = 15000K$. (d) $T_{tr} = 10000K$.

Figure 10. Vibrational distribution of N_2 molecules in QSS for $T_{tr} = 30000K, 20000K, 150000K$ and $10000K$ for the $N + N_2$ and $N_2 + N_2$ processes

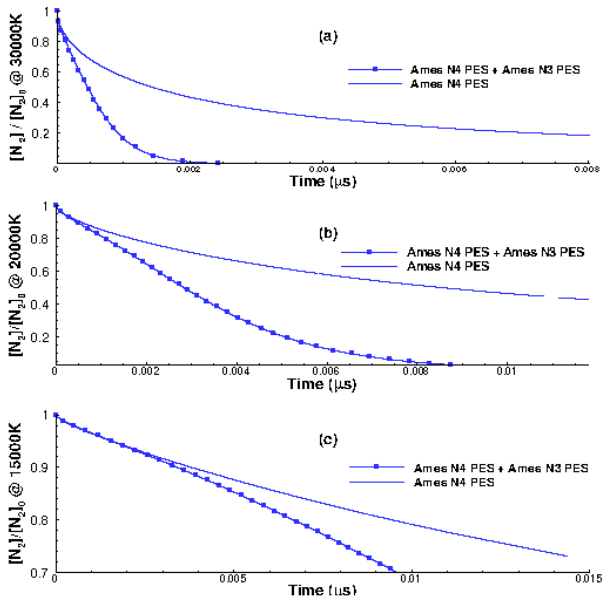

Figure 11. Composition history comparison for N3+N4 system and N4 system.

the N4 processes between the two PESs. In this section we will compare the combined N3+N4 process for isothermal relaxation of nitrogen for the two PESs.

For the comparative study, three cases were analyzed and can be seen in Fig. 12. For the first two cases shown in Fig.12(a) and 12(b) the isothermal box relaxation was initialized with the system containing nitrogen molecules at $T_{rot} = T_{vib} = 3000$K with no atomic nitrogen present. In these cases the translational temperature was set to $T_{tr} = 30000$K and $T_{tr} = 20000$K respectively. As the system evolves, we see dissociation of molecular nitrogen and excitation of internal energy modes to QSS levels. The excitation curves and the QSS temperatures for the internal energy modes given by both the PESs are identical and the composition history of molecular nitrogen is comparable. The third case presented here is for $T_{tr} = 10000$K. Here the isothermal box relaxation was initialized with nitrogen molecules having $T_{rot} = T_{vib} = T_{tr}$ and with no atomic nitrogen present. For this case too, we find that the two PESs predict the same QSS temperatures but we do see that the Ames PES result is more dissociative than that for the UMN PES. A similar trend was observed for the N4 case at $T_{tr} = 10000$K.[20] At this time we would like to re-iterate that temperatures presented here are actually measures of average energy and have been defined in Sec. II D.

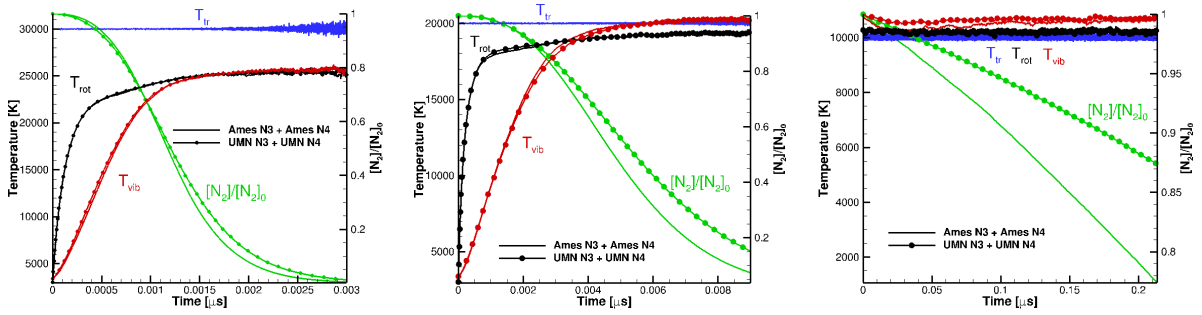

(a) $T_{tr} = 30000K$. (b) $T_{tr} = 20000K$. (c) $T_{tr} = 10000K$.

Figure 12. Composition and temperature history comparison for N3+N4 system using the Ames PES[3,23,24] and the UMN PES.[4,5] For $T_{tr} = 30000K, 20000K, 150000K$ and $10000K$

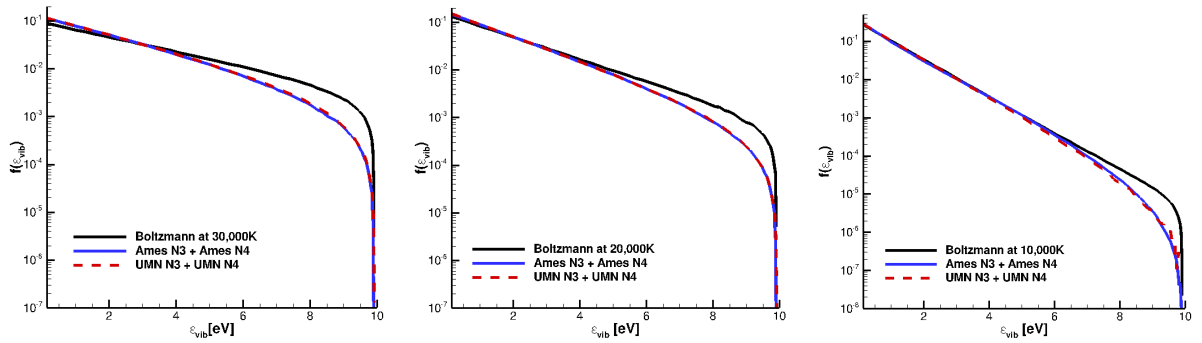

(a) $T_{tr} = 30000K$. (b) $T_{tr} = 20000K$. (c) $T_{tr} = 10000K$.

Figure 13. Vibrational distribution of N_2 molecules in QSS for $T_{tr} = 30000K, 20000K$ and $10000K$ for the $N + N_2$ and $N_2 + N_2$ processes

In Fig 13 we present the QSS vibrational energy distribution functions for the cases shown in Fig. 12. The QSS vibrational energy distributions given by the two PESs are identical. This shows that the results produced by the two PESs agree at the at the molecular level as well.

IV. Conclusions

DMS calculations, using PESs developed at NASA Ames Research Center were performed for dissociating nitrogen systems. It was found that for the $N + N_2$ process the characteristic vibrational excitation times are an order of magnitude lower than those predicted by the Millikan and White correlation. At the molecular level, it was observed that during vibrational excitation the high energy tail of the vibrational distribution becomes over populated first and as the system evolves the lower energy levels get populated.

For the dissociation phenomenon it was observed that the dissociation proceeds more rapidly for the $N + N_2$ process compared to only $N_2 + N_2$ processes. At the molecular level it was found that the probability of dissociation goes as $1/T_{tr}$ for molecules with $\epsilon_{int} < 9.9eV$. For molecules with $\epsilon_{int} > 9.9eV$ (quasi-bound molecules) the probabilities of dissociation become weakly dependent on translational temperature. One can extend the above conclusion to say that the dissociation of quasi-bound molecules is weakly dependent on the translational energy of the collision partner. It should be noted that the non-equilibrium dissociation rate coefficients obtained match up with the extrapolation proposed by Appleton *et al.* based on experimental data.

Lastly, we have seen that the characteristic vibrational excitation times and non-equilibrium dissociation rate coefficients calculated using the Ames PES and the UMN PES are comparable. Additionally, the non-equilibrium dissociation rate coefficients obtained from both the PESs agree well with the extrapolations based on experimental data presented by Appleton *et al.*. Finally, as seen in Sec. III D for the combined N3+N4 process the rotational and vibrational temperatures in QSS and vibrational energy distributions in QSS given by the two PESs are identical and the composition histories given by the two PESs are comparable. Given that the two independently developed PESs give results that agree fairly well lends confidence in using computational chemistry in hypersonic applications.

V. Acknowledgements

The research presented is supported by Air Force Office of Scientific Research (AFOSR) under Grant No. FA9550-16-1-0161. The views and conclusions contained herein are those of the authors and should not be interpreted as necessarily representing the official policies or endorsements, either expressed or implied, of the AFOSR or the US government. The authors would like to thank Dr. Michael Barnhardt and Dr. David Hash at NASA's Ames Research Center for providing the opportunity for collaboration between Ames Research Center and the University of Minnesota. Maninder Grover was supported by the Doctoral Dissertation Fellowship at the University of Minnesota.

References

[1]J. P. Appleton, M. Steinberg and D. J. Liquornik, Shock-Tube Study of Nitrogen Dissociation using Vacuum-Ultraviolet Light Absorption, J. Chem. Phys. 48 (2), 599- 608 (1968).

[2]R.K. Hanson and D. Baganoff, "Shock-tube study of nitrogen dissociation rates using pressure measurements", AIAA Journal, 10(2), Feb. 1972.

[3]R. L. Jaffe, D. W. Schwenke, G. Chaban, Vibrational and Rotational Excitation and Dissociation in N2-N2 Collisions from Accurate Theoretical Calculations, AIAA Thermophysics and Heat Transfer Conference, 28 June-1 July 2010, Chicago, IL, AIAA 2010-4517.

[4]Y. Paukku, K. R. Yang, Z. Varga, and D. G. Truhlar, Global ab initio ground-state potential energy surface of N4, J. Chem. Phys. 139, 044309 (2013); erratum ibid., 140, 019903 (2014).

[5]J. D. Bender, P. Valentini, I. Nompelis, Y. Paukku, Z. Varga, D. G. Truhlar, T. E. Schwartzentruber, and G. V. Candler. An improved potential energy surface and multi-temperature quasiclassical trajectory calculations of N2 + N2 dissociation reactions. The Journal of Chemical Physics, 143(5):054304, 2015.

[6]D. G. Truhlar and J. T. Muckerman. Atom-Molecule Collision Theory: A Guide for the Experimentalist, page 505. Plenum, 1979.

[7]Gert Due Billing and E.R. Fisher. VV and VT rate coefficients in N2 by a quantum-classical model. Chemical Physics, 43(3):395 401, 1979.

[8]F. Esposito, I. Armenise, and M. Capitelli. N-N2 state to state vibrational-relaxation and dissociation rates based on quasi-classical calculations. Chem. Phys., 331(1):1 8, 2006.

[9]F. Esposito and M. Capitelli. Quasiclassical molecular dynamic calculations of vibrationally and rotationally state selected dissociation cross-sections: $N + N_2 \rightarrow 3N$. Chemical Physics Letter 302(12):49-54, 1999

[10]Marco Panesi, Richard L. Jaffe, David W. Schwenke, and Thierry E. Magin. Rovibrational internal energy transfer and dissociation of N2(1Σ g +)-N(4 S u) system in hypersonic flows. The Journal of Chemical Physics, 138(4):044312, 2013.

[11]J.G. Kim and I.D. Boyd. State-resolved mater equation analysis of thermochemical non-equilibrium of nitrogen. Chemical Physics, 138(4):044312, 2013

[12]G.A. Bird, "Molecular Gas Dynamics and Simulation of Gas Flows", Clarendon, Oxford, 1994

[13]K. Koura. Monte Carlo direct simulation of rotational relaxation of diatomic molecules using classical trajectory calculations: nitrogen shock wave. Phys. Fluids, 9(11):35433549, 1997.

[14]K. Koura. Monte Carlo direct simulation of rotational relaxation of nitrogen through high total temperature shock waves using classical trajectory calculations. Phys. Fluids, 10(10):26892691, 1998.

[15]H. Matsumoto and K. Koura. Comparison of velocity distribution functions in argon shock wave between experiments and Monte Carlo calculations for Lennard-Jones potential. Phys. Fluids, 3(12):30383045, 1991.

[16]Paul Norman, Paolo Valentini, and Thomas Schwartzentruber. GPU-accelerated classical trajectory calculation direct simulation Monte Carlo applied to shock waves. Journal of Computational Physics, 247(0):153 167, 2013.

[17]P. Valentini, P. Norman, C. Zhang, and T. E. Schwartzentruber. Rovibrational coupling in molecular nitrogen at high temperature: An atomic-level study. Physics of Fluids, 26(5):056103, 2014.

[18]Grover, M.S., Valentini, P, and Schwartzentruber, T.E., Coupled rotational-vibrational excitation in shock waves using trajectory-based direct simulation Monte Carlo, AIAA Paper 2015-1656, Jan. 2015, presented at the 53rd Aerospace Sciences Meeting, AIAA SciTech, Kissimmee, FL.

[19]P. Valentini, T. E. Schwartzentruber, J. D. Bender, I. Nompelis, and G. V. Candler. Direct molecular simulation of nitrogen dissociation based on an ab initio potential energy surface. Physics of Fluids, 27(8):086102, 2015.

[20]Jaffe, R.L., Schwenke, D. W., Grover, M.S., Valentini,P., Schwartzentruber, T.E., Venturi, S., and Panesi.M., "Comparison of quantum mechanical and empirical potential energy surfaces and computed rate coefficients for N2 dissociation", 54th AIAA Aerospace Sciences Meeting, AIAA SciTech 2016, (AIAA 2016-0503)

[21]P. Valentini, T. E. Schwartzentruber, J. D. Bender, and G. V. Candler, "Dynamics of nitrogen dissociation from direct molecular simulation" Phys. Rev. Fluids 1, 043402 (2016)

[22]D. Frenkel and B. Smit. Understanding Molecular Simulation. Academic Press, 2002.

[23]G. Chaban,R. L. Jaffe, D. W. Schwenke and W. M. Huo, "Dissociation cross sections and rate coefficients for nitrogen from accurate theoretical calculations", AIAA 2008-1209, 2008

[24]R. L. Jaffe, D. W. Schwenke and G. Chaban, "Theoretical analysis of N2 collisional dissociation and rotation-vibration energy transfer", AIAA 2009-1569, 2009

[25]C. Park, Assessment of a two-temperature kinetic model for dissociating and weakly ionizing nitrogen, Journal of Thermophysics and Heat Transfer 2, 816 (1988).

[26]C. Park, Review of chemical-kinetic problems of future nasa missions. i-earth entries, Journal of Thermophysics and Heat transfer 7, 385398 (1993).

[27]R. L. Jaffe, The calculation of high-temperature equilibrium and nonequilibrium specific heat data for n2, o2 and no, in 22nd AIAA Thermophysics Conference, Honolulu, Hawaii AIAA-1987-1633

[28]L. I. Schiff, "Quantum Mechanics", 3^{rd} edition. McGraw-Hill, New York (1955)

[29]R.C. Millikan and D. R. White, "Systematics of vibrational relaxation". The Journal of Chemical Physics, 39(12):3209-3213, 1963.

[30]C. Park, J. T. Howe, R. L. Jaffe, and G. V. Candler, Review of a chemical kinetic problem of a future NASA mission. II. Mars entries, J. Thermophys. Heat Transfer, 8, No. 1, 923 (1994).